



## Emission enhancement in nanoassemblies with extremely small metal nanoparticles: Nonmonotonic effect of temperature and the non-Markovian interactions

Riya Dutta <sup>1</sup>, Kritika Jain,<sup>2</sup> Komal Sharma <sup>1</sup>, Murugesan Venkatapathi <sup>2</sup> and J. K. Basu<sup>1,\*</sup>

<sup>1</sup>*Department of Physics, Indian Institute of Science, Bangalore 560012, India*

<sup>2</sup>*Computational and Statistical Physics Laboratory, Indian Institute of Science, Bangalore 560012, India*

 (Received 8 April 2023; revised 30 August 2023; accepted 9 October 2023; published 30 October 2023)

Compact light-emitting quantum dot monolayers find wide-ranging applications in photovoltaics to display technology. A key aspect of display technology is the light extraction capability and the quantum efficiency of these layers. The usual Purcell enhancement requiring large-scale proximal metal nanostructures would completely disrupt the packing of such ordered layers and hence cannot be used. In this report, we demonstrate a nonmonotonic temperature dependence of emission enhancement in compact tiny, fully absorbing metal nanoparticle embedded quantum dot layers, which is captured by a non-Markovian treatment of emitter-metal nanoparticle interactions. We also demonstrate how this nonmonotonic behavior with temperature is dominated by the electron-phonon interactions in the metal nanoparticles. Significantly, the observed photoluminescence enhancement maximum of  $\sim 10$  occurs at a temperature of  $\sim 150$  K which is much higher compared to earlier reports. The results suggest the possibility of using our platform in various display, photonic, and sensing devices with higher sensitivity and energy efficiency.

DOI: [10.1103/PhysRevMaterials.7.105201](https://doi.org/10.1103/PhysRevMaterials.7.105201)

### I. INTRODUCTION

Nanoparticles (NPs) offer tunable and strong optical [1–6] properties as their shape-sensitive resonances produce large optical cross sections. Such resonances have been used for various applications in sensing or imaging [7–9]. Several studies have also shown that these resonances can be used to tailor spontaneous emission (SE) of emitters placed in close proximity to the NPs [10–12]. From an application point of view, the enhancement of SE is vital because it can enable highly efficient light-emitting devices [13,14], low-threshold lasers [15,16], and highly efficient single photon sources [17–19]. The spontaneous emission of a photon from an excited atom or a molecule remains unaffected by an object placed at distances much larger than the wavelength. A quantum interaction regime is especially significant when a micro/nanoscale object with strong optical resonances is placed at distances less than the emission wavelength. A highly scattering body with efficiencies  $\gg 1$ , placed at the appropriate distances, adds to the radiative decay rate and the probability of photon emission, while an absorbing body increases the nonradiative decay of the emitter-matter system [20]. This gainful (Purcell) effect due to a weak coupling of the larger highly scattering plasmonic particles ( $> 50$  nm in sizes) has been verified by many experiments [21–23].

Recently, anomalous enhancements of spontaneous emission near fully absorbing metal nanoparticles less than 10 nm in dimensions that do not scatter light were reported [24–29]. A marginal effect on their permittivity (i.e., minor oscillations and shifts in spectra) due to the scattering of electrons at the

boundaries of these small particles have been known. However, they do not explain the above anomalous enhancements of radiative decay [30–36]. Because the dissipation rates in the smaller metal nanoparticles are low, it can result in stronger coupling strengths even at large relative separations. Hence, even the moderate to strong coupling regime of such systems might require non-Markovian methods to model the radiative and nonradiative decays. In the Markovian regime, interactions can be represented by a memory-less chain of events, and this is especially appropriate when a system interacts with a much larger entity in terms of its size or the density of its possible states, i.e., a bath. A non-Markovian behavior, on the other hand, typically involves closed loops of interactions among the two systems, and in the case of quantum systems, the required superpositions of many such interactions may be nontrivial to study [37–40]. Strong coupling between quantum emitters and cavities can result in exponentially damped oscillatory decays that characterize this non-Markovian decay [41–43]. The effect of such interactions of an emitter with a metal surface on the total decay and the effective Rabi frequencies have been elucidated earlier [44,45]. A model for the oscillatory dynamics of excitation energy transfer was proposed as well [46]. Earlier, a one-loop correction was suggested to re-normalize the conventional partition of the total decay into its radiative and nonradiative decay components [28,47,48], to account for non-Markovian effects at moderate coupling strengths.

Recent work also presented a non-Markovian model to evaluate the expected radiative and nonradiative decays of emitters with stronger couplings to such nanostructures [49]. It has been reported that the quantum efficiency of emitter assemblies can further be enhanced by reducing temperature [50]. However, such enhancements can be achieved

\*basu@iisc.ac.in

at cryogenic temperatures, making it unsuitable for device applications. Further, such studies have focused on using large metal nanoparticles, which limits them to the temperature dependence of the conventional Purcell effect. It would thus be pertinent to explore if the temperature dependence of smaller metal nanoparticle-based system, as reported by us earlier [25,28,51], follows similar behavior to that observed with large metal nanoparticles. The main reason why the weak matter-coupling (Purcell) regime of emission enhancement has not impacted most applications in the light generation is the large volume of precious noble metals required as highly scattering nanoparticles  $\sim 100$  nm in dimensions. This drawback may be significantly mitigated by similar enhancements that are possible using a comparable number of fully absorbing tiny nanoparticles ( $< 10$  nm in size), thus reducing the volume of metals required by large factors. In fact, it might be possible to take further advantage of the reported enhancement of quantum efficiency of such emitter assemblies by reducing temperature [50]. While going to lower temperatures might help reduce the dissipative losses mainly due to electron-phonon coupling, an important question remains as to whether the energy losses in the plasmon damping can be reduced further without impacting the overall strength of the non-Markovian coupling of the metal nanoparticle. At lower temperatures, note that most of the losses may be due to the electron-electron interactions rather than the electron-phonon interactions in the metal particle.

In this report, we elucidate the modulating effect of the electron-phonon interactions on the non-Markovian coupling with the metal nanoparticles using low temperature photoluminescence (PL) experiments. Temperature-dependent photoluminescence (PL) data collected from compact monolayer films of semiconducting light-emitting quantum dots (QDs) embedded with tiny gold nanoparticles (diameter  $< 5$  nm), revealing, a non-monotonic temperature-dependent PL enhancement with a maximum at 150 K. The experimental results are modeled by numerical calculations suggesting that the maximum gains of the non-Markovian nanoparticle-based resulting enhancements are possible at  $\sim 150$  K, where the coupling of the electrons with the low energy phonons may dominate over the dissipative effects of the electron-electron interactions. We also demonstrate how this temperature dependence is essentially driven by the electron-phonon interactions with the intriguing observation that the crossover temperature of  $\sim 150$  K is very close to the Debye temperature,  $T_D$ , of gold nanoparticles [52,53]. The results suggest strategies to further enhance emission efficiencies in such emitter assemblies through temperature tuning, which can be very useful for their optoelectronic applications.

## II. EXPERIMENTAL DETAILS

The experimental results presented here are based on DDT-capped AuNP embedded OA-capped CdSe-ZnS core-shell QD monolayer film [28,51,54]. The details of the quantum dot and metal nanoparticle synthesis are provided in the Supplemental Material (SM) [55]. The mean diameter of QDs are  $6.7 \pm 0.5$  nm, and that of AuNPs are  $3.8 \pm 0.6$  nm as

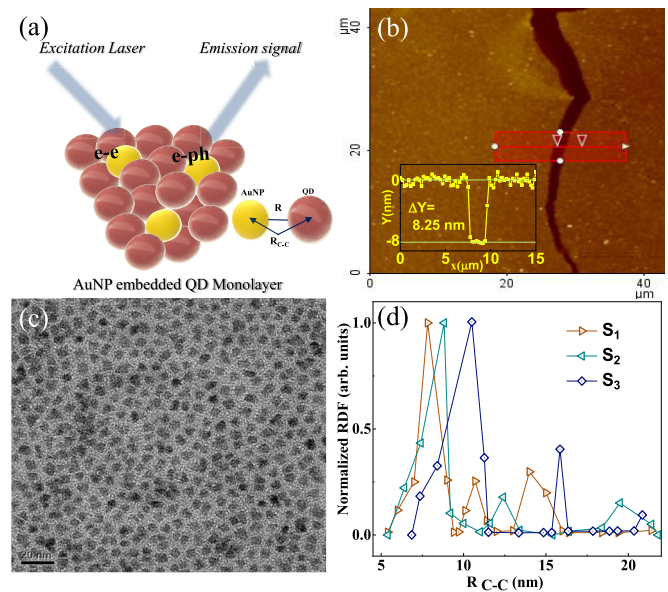


FIG. 1. (a) Schematic representation of the experimental system involving compact assemblies of quantum dots (QDs, red spheres) and gold nanoparticles (AuNP, yellow spheres).  $R$  represents the average surface separation between QDs and AuNPs. (b) The AFM topographical image of an AuNP embedded QD film ( $S_2$ ) inset shows the corresponding layer height, estimated from a breakage in the compact layer. (c) TEM images of  $S_2$  film. (d) The surface separation between the QD and AuNP,  $R$ , has been obtained from radial distribution function (RDF) calculation from TEM images of the different systems.

obtained from TEM images as shown in Figs. 1 and 2 in the SM [55]. Considering their strong plasmonic response [56], AuNPs are incorporated in the compact QD monolayer film

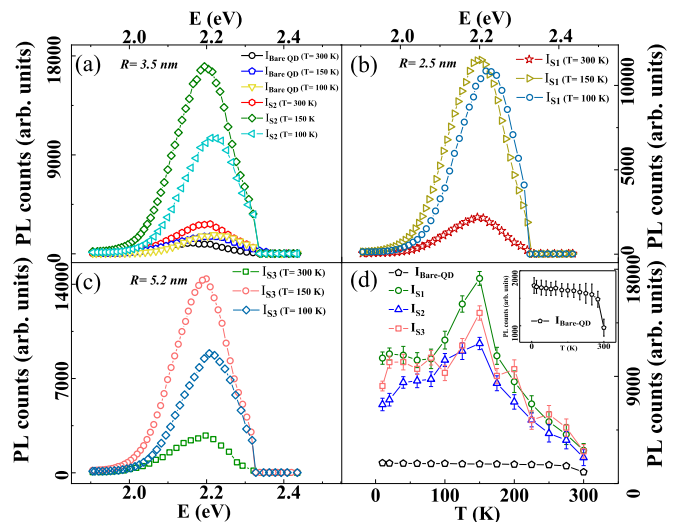


FIG. 2. (a) PL emission spectrum from bare QD and AuNP embedded QD films at  $T = 100$  K, 150 K, and 300 K for the system  $S_2$ . Respective PL emission spectrum for the system (b)  $S_1$  and (c)  $S_3$ . (d) The PL intensity counts as a function of temperature for bare (inset) and AuNP embedded QD films,  $S_1$ ,  $S_2$ ,  $S_3$ . Error bars have been calculated based on multiple measurements. The QD monolayer shows an expected monotonic increase in PL intensity with decreasing temperature (inset).

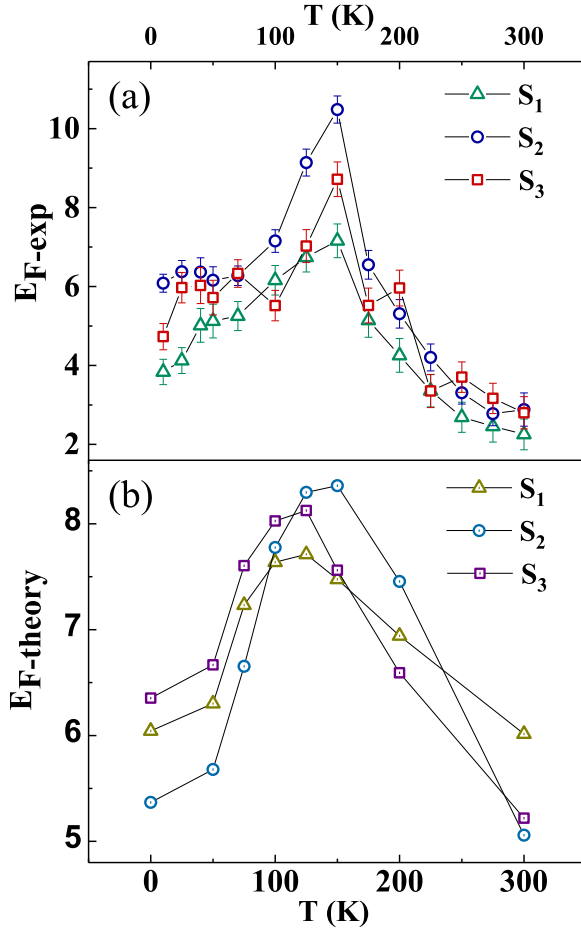


FIG. 3. (a) Temperature dependent enhancement factor ( $E_{F-exp}$ ) for different surface separation  $R$ . Error bars have been calculated based on multiple measurements. (b) Theoretically calculated emission enhancement factor ( $E_{F-theory}$ ) for the similar surface separation. Note that in conventional theory a small nonscattering particle does not produce enhancements.

having a number ratio (1 : 6) using the Langmuir-Blodgett (LB) technique discussed earlier [57–60] (see Fig. 3 of the SM). The mutual interaction depends on the surface separation ( $R$ ) between the QD to AuNP, which is determined by surface ligand lengths in a compact structure. In experimental conditions,  $R$  has been varied over a range of 2.5 nm to 5.2 nm using different capping ligands (see the SM).  $S_1$ ,  $S_2$ , and  $S_3$  are three different systems having surface separations of  $R = 2.5$  nm, 3.5 nm, and 5.2 nm have been picked up for this particular systematic study. Temperature-dependent photoluminescence (PL) measurements of the samples were performed using a Horiba PL setup using a closed-cycle Helium cryostat. The emission path was coupled to the spectrometer via an optical interface. A 532 nm laser was used as an excitation source for PL measurements. Incident power of the laser has been kept fixed  $2 \mu\text{W}/\text{cm}^2$ , and the integration time for the PL spectra was set to one second (with five accumulations). The PL spectra were collected in reflection mode using a  $50\times$  objective. The laser spot size diameter is approximately 900 nm, resulting in an illuminated area of roughly  $1.27 \mu\text{m}^2$ . Measurements were conducted on multiple

samples, including AuNPs-doped QD and bare QD samples. Multiple regions were scanned within each sample, and several point spectra were collected.

### III. THEORETICAL METHODS

The full non-Markovian interaction model already presented elsewhere [49] was combined with a temperature dependent permittivity to predict the variation of emission with temperature. To include the effects of non-Markovian interactions, first we construct a mixture of initial states to represent the coupled system where the photon can also be re-absorbed by the emitter from the metal nanoparticle. This was done by decomposing the emitter-particle system into many dipole granules and evaluating their mutual self-interactions. The collective eigenstates and corresponding self-energies of the excited system were used to construct a density matrix  $\rho$  for the system. Second, to obtain the superposition of radiative decay over all the oscillators in an excited initial state and the ensemble of such initial states, we decomposed this mixture into a set of orthogonal pure states  $\phi^i$ . This allows us to sum over the superposition of the radiative decay from the oscillators in each orthogonal state to evaluate the expected  $\Gamma^r$ . Solving Hermitian eigenvalue problems  $\rho|\phi^i\rangle = p_i|\phi^i\rangle$ , we have probabilities  $p_i$  and the pure states  $\phi^i$  in the mixture.

The expected radiative decay rate of the system is given by  $\langle \Gamma^r \rangle = \sum_{i=1}^n p_i \Gamma_i^r$ . The quantum efficiency is given by  $Q = \frac{\langle \Gamma^r \rangle}{\Gamma^{total}}$ . The temperature dependent permittivity is described as [61]

$$\varepsilon(T) = \varepsilon_\infty - \frac{\omega_p^2(T)}{\omega(\omega + i\omega_c(T))}, \quad (1)$$

where  $\omega$  is the angular frequency of incoming wave,  $\varepsilon_\infty$  is high-frequency permittivity of Au,  $\omega_p$  is temperature dependent plasmon frequency described below and  $\omega_c$  is the collision frequency which includes both electron-electron  $\omega_{e-e}(T)$  and electron-phonon contributions  $\omega_{e-ph}(T)$ , i.e.,  $\omega_c(T) = \omega_{e-e}(T) + \omega_{e-ph}(T)$ . These contributions are described as

$$\omega_p(T) = \frac{\omega_p(T_0)}{\sqrt{1 + 3\gamma(T - T_0)}}, \quad (2)$$

$$\omega_{e-e}(T) = \frac{\pi^3 \Gamma \Delta}{12 \hbar E_F} \left[ (k_B T)^2 + \left( \frac{\hbar \omega}{2\pi} \right)^2 \right], \quad (3)$$

$$\omega_{e-ph}(T) = \omega_0 \left[ \frac{2}{5} + \frac{4T^5}{\theta_D^5} \int_0^{\frac{\theta_D}{T}} \frac{z^4}{e^z - 1} dz \right], \quad (4)$$

where  $T_0$  is the room temperature (300 K),  $\hbar$  is the Planck's constant,  $k_B$  is the Boltzmann constant,  $\theta_D$  is the Debye's temperature,  $E_f$  is the Fermi energy for Au,  $\Gamma$  is the Fermi-surface average of scattering probability,  $\gamma$  is the thermal linear expansion coefficient, and  $\Delta$  is the fractional Umklapp scattering coefficient. We took  $\varepsilon_\infty = 1$  here, and all other quantities are taken from the reported study [61].

This temperature dependent permittivity was also further decomposed into the components due to electron-phonon interactions and electron-electron interactions, considering  $\omega_c = \omega_{e-ph}$  and  $\omega_c = \omega_{e-e}$  in Eq. (1), respectively, allow-

ing deeper insights into this behavior. The contribution from electron-phonon interactions dominates electron-electron interactions by an order of magnitude. The variations of these contributions with temperature is plotted in Fig. 9 of the SM. More details on the theoretical methods are provided in the SM [55] (see also Refs. [49,62–68]).

#### IV. RESULTS AND DISCUSSION

In a recent study [28], we reported the unexpected large Purcell enhancements in compact quantum dot assemblies embedded with tiny gold nanoparticles, with a nonmonotonic dependence on the quantum dot-metal nanoparticle separation,  $R$ . Our findings from theoretical model calculation demonstrated that when dealing with finite size emitters at small separations, the commonly used point emitter approximations deviate from the actual observations [69]. Also, this unexpected behavior was explained in terms of non-Markovian interactions under one-loop corrections [47,48], whereas the emission enhancements due to larger highly scattering particles were evident even in the Markovian models suited for weak coupling. In this study, we investigate the temperature-dependent behavior of photoluminescence (PL) emission in compact assemblies of quantum dots (QDs) that are embedded with small AuNPs, similar to our previous study [28]. Here, we focus on the surface separations  $R$  values, where the maximum enhancements were observed earlier.

Figure 1(a) presents the schematic diagram of the experimental system. The mean surface separation between the QD and AuNP is defined as  $R$ . We have varied the separation by varying the ligand attached to the QD and AuNP surface. The system was probed using laser excitation of energy 2.33 eV, and the response signal was collected normally to the plane of the sample. Here, we study the interplay between the electron-electron (e-e) and electron-phonon (e-ph) interactions governing the emission enhancement in these systems. Atomic force microscopy (AFM) and transmission electron microscopy (TEM) images for the sample  $S_2$  with  $R = 3.5$  nm, presented in Figs. 1(b) and 1(c), respectively, confirm the compact arrangement of the QD film embedded with AuNP in the planar structure. The height of the monolayer was estimated to be  $\sim 8.25$  nm from typical height profiles in the AFM image in Fig. 1(b), which is in agreement with the diameter of the nanoparticles as obtained from TEM images, including the capping ligand lengths. The mean surface separation ( $R$ ) was obtained from the radial distribution function (RDF) estimated from the TEM images of the hybrid films as shown in Fig. 1(d). As summarized in Table I,  $S_1$ ,  $S_2$ , and  $S_3$  correspond to the mean  $R$  of 2.5 nm, 3.5 nm, and 5.2 nm, respectively. TEM images for  $S_1$  and  $S_3$  films are provided in the SM (Fig. 4).

Temperature dependent PL measurements of CdSe/ZnS QDs [70,71] in particular and semiconducting QDs have been widely reported in the literature [72], and it is known that in general the emission intensity increases as the temperature is reduced. This increase in emission intensity has been attributed to the reduction in phonon dissipation at lower temperatures [71].

Figure 2(a) displays the PL spectra of the AuNP embedded  $S_2$  film and the reference QD film at temperatures 300 K,

TABLE I. Sample Details.

System index <sup>a</sup>	Ligand details	$R_{C-C}$ (nm)	$R$ (nm)
$S_1$	EDT-QD and EDT-AuNP	7.75	2.5
$S_2$	OA-QD and DDT-AuNP	8.75	3.5
$S_3$	OA-QD and ODT-AuNP	10.45	5.2

<sup>a</sup>The table shows the sample indexes of AuNP-embedded QD films where  $S_1$ ,  $S_2$ , and  $S_3$  systems are differed by different ligands attached to QDs and AuNPs that leads to nonidentical  $R$  values. Here, we have considered  $R_{C-C}$  as the center-to-center distance between two nanoparticles, whereas  $R$  is defined as the separation between the surfaces of those particles.

150 K, and 100 K. Interestingly, the PL intensity of the AuNP embedded QD monolayer is maximum at an intermediate temperature of 150 K. On the other hand, the PL intensity variation of the reference QD film shows a monotonic increase with decreasing temperature consistent with earlier observations [73]. The QD monolayer also shows a blue shift in the energy of the PL maxima with decreasing temperature as expected from the Varshni equation [74] (see Fig. 5 of the SM). A similar nonmonotonic PL response with temperature was also observed for  $S_1$  and  $S_3$  systems presented in Figs. 2(b) and 2(c). In Fig. 2(d), we summarize the complete temperature dependence of the PL of all samples  $S_1$ ,  $S_2$ , and  $S_3$ , as well as the QD monolayer sample.

While the QD monolayer shows an expected monotonic increase in PL intensity with decreasing temperature, as shown in the inset of Fig. 2(d), the variation is strikingly nonmonotonic for the different AuNP embedded QD monolayers. We did not observe any substantial variation in the maximum temperature for samples with different  $R$  values reaching a maximum at a temperature of  $\sim 150$  K in contrast to the

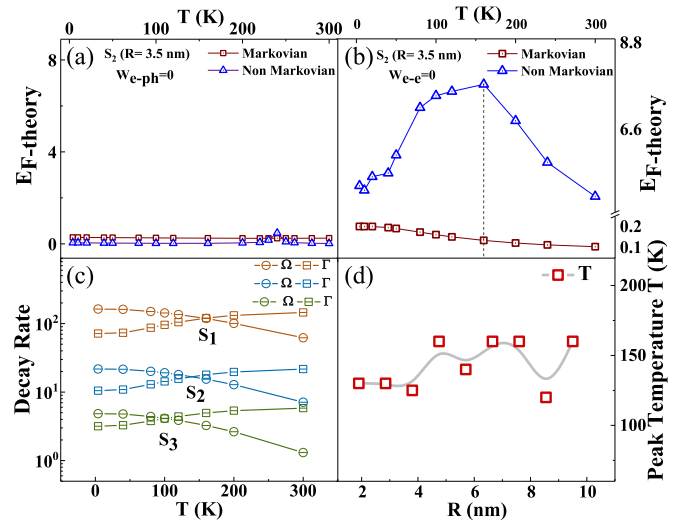


FIG. 4. (a) Emission enhancement factor ( $E_{F-theory}$ ) for Markovian and non-Markovian models with vanishing electron-phonon interactions ( $W_{e-ph} = 0$ ) and (b) electron-electron interactions ( $W_{e-e} = 0$ ). (c) Rabi frequency ( $\Omega$ ) and total decay rate ( $\Gamma$ ), in units of the vacuum decay rate of the isolated emitter ( $\Gamma_0^r$ ), varying as a function of temperature ( $T$ ). (d) Peak temperature values at which PL intensity maximizes for different surface separation  $R$ .

monotonic PL intensity trend for the QD monolayer. We have conducted measurements on multiple samples, approximately ten in total, for both bare QD and AuNP-embedded QD samples. Multiple regions were scanned within each sample, and several point spectra were collected. Notably, these results exhibited a high level of consistency in terms of QD size and QD-AuNP spacing. A series of spectra collected from multiple bare QD and AuNP-embedded QD film at  $T=150$  K (see Fig. 6 of the SM) shows the PL counts variation over samples.

To further analyze the PL emission behavior, the enhancement factor ( $E_F$ ) has been calculated as the ratio of the PL intensity of the AuNP-QD hybrid film ( $I_{\text{AuNP-QD}}$ ) to that of the bare QD film ( $I_{\text{bare-QD}}$ ) at a given temperature, as shown in Equation:

$$E_{F\text{-exp}} = \frac{I_{\text{AuNP-QD}}}{I_{\text{bare-QD}}} \quad (5)$$

Figure 3(a) shows the nonmonotonic variation of the  $E_{F\text{-exp}}$  with temperature for three different experimental systems  $S_1$ ,  $S_2$ , and  $S_3$  corresponding to surface separation between emitters and AuNPs,  $R$ , of 2.5, 3.5, and 5.2 nm respectively. The  $E_{F\text{-exp}}$  monotonically increases with decreasing temperature from a value of  $\sim 3$  to a maximum of around  $\sim 11$  at 150 K. With a further decrease in temperature,  $E_{F\text{-exp}}$  decreases further down to 4 K, although it remains higher as compared to its value at room temperature. To gain a better understanding of the underlying mechanisms, theoretical calculations of the Purcell factor have been performed using both Markovian and non-Markovian models, taking into account the temperature-dependent dielectric function of the AuNP embedded films.

Figure 3(b) summarizes the enhancement factor ( $E_{F\text{-theory}}$ ) obtained from the model calculations, and the variation over temperature exhibits similar non-monotonic behavior with enhancement factors of the order of ten as experimental observations show in Fig. 3(a). The non-Markovian interactions between the emitter and the small, fully absorbing metal nanoparticle (i.e., with negligible scattering) are suspected to be responsible for significant enhancements in spontaneous emission and the nonmonotonic trend of the enhancement factors with temperature.

The strength of emitter-to-plasmon coupling is predominantly influenced by the phonon contribution, which is more sensitive to the system temperature. To elucidate the underlying mechanism behind the nonmonotonic temperature dependence of photoluminescence (PL) enhancement, we employed a non-Markovian model that considers the interaction between emitters and metal nanoparticles. In this work, we combined the full non-Markovian interaction model [49] with a temperature-dependent permittivity [61] to predict the temperature variation of emission. We further decomposed the temperature-dependent permittivity into its components due to electron-phonon and electron-electron interactions, enabling us to understand this behavior better. Our non-Markovian model revealed that the radiative decay increases and nonradiative loss decrease in comparison to conventional Markovian models. Figures 4(a) and 4(b) depict the predicted enhancement factor for emission as a function of temperature by considering the two contributions of interaction, namely electron-electron (e-e) and electron-phonon (e-ph) in-

teractions. To understand the individual contribution of these interactions to the overall effect, we calculated them independently. First, we neglected the e-ph contribution and observed that the enhancement factor due to e-e interaction remained almost constant over the temperature variation [Fig. 4(a)]. On the other hand, when we ignore the e-e interactions, we observe a nonmonotonic variation of enhancement on account of e-ph interaction [Fig. 4(b)]. Additionally, we found that the contribution from e-ph interactions dominates over e-e interactions by order of magnitude. Figure 4(c) shows the variations of the Rabi frequency ( $\Omega$ ) and total decay rate ( $\Gamma$ ) with temperature for three different surface separations ( $R$ ). The increase in Rabi frequencies ( $\Omega$ ) and decay rates ( $\Gamma$ ) vary sharply (as  $R^{-6}$ ) between  $S_3$  and  $S_1$ . But note that the coupling strength (ratio of  $\Omega$  and  $\Gamma$ ) varies more slowly with separations, and this determines the overall variations of the observed enhancements. It provides deeper insight into nonmonotonic behavior shown in Fig. 4(b), highlighting that moderate coupling strengths can result in reduced dissipation and larger enhancements. Figure 4(d) summarizes the theoretically calculated maximum enhancement temperature as a function of different surface separations,  $R$ . The data shows that the temperature of the maximum PL enhancement is relatively insensitive up to a  $R$  value of 10 nm. At room temperature, quantum yield (QY) enhancement has been analyzed and compared between various experimental and theoretically calculated systems for varying surface separations,  $R$  (see Fig. 7 of the SM). Now, the temperature-dependent variations of the radiative decay rate ( $\Gamma_r$ ) and quantum efficiency (QE) have been presented in the SM (see Fig. 8). The maximum value of both  $\Gamma_r$  and QE is achieved at a specific surface separation ( $R = 3.8$  nm), beyond which they decrease for longer separations. The large PL enhancements observed with tiny, fully absorbing metal nanoparticles in our current work for various values of  $R$  are consistent with our earlier results [28] at room temperature. However, the most significant observation in this work is the emergence of an intermediate temperature regime of maximum PL enhancement. So what explains the emergence of this intermediate temperature regime of PL enhancement? It is clear that e-ph interactions are the dominant contribution to the dissipation in the metal nanoparticle at room temperature. With the reduction in temperature, this dissipation reduces due to the annihilation of high energy phonon modes which overcomes the possible reduction in non-Markovian interaction strengths leading to an increase in PL enhancement. This regime persists until  $\sim 150$  K, which is very close to the Debye temperature of gold. Below this temperature regime, a combination of increasing effects of e-e interaction mediated dissipation, coupled with the reduction in non-Markovian coupling with low-frequency phonon modes, more than compensates for the reduced dissipation due to e-ph interaction, leading to reduced emission intensities.

Nevertheless, the theoretical model is still a coarse approximation if one considers the other parameters ignored, such as variable separations and shapes of NPs in the actual film. More importantly, the finite size of the emitters is in the same order as the separations with the NP, meaning that our theoretical results using a point emitter are not suited for fitting experimental results directly. It is more useful for qualitative

predictions as a function of the size of the NP, the separations, and the permittivity of the NP. Also, note that the ordering of the peaks of  $S_1$ ,  $S_2$ , and  $S_3$  (different mean separations) for the varying temperatures is identical in the theoretical and experimental results showing the reliability of the semiquantitative predictions. Increased control of parameters in experiments and inclusion of other parameters in the theoretical model may be required for exact replication of the experimental results in the simulations.

Note that the non-Markovian interaction (with possible re-absorption of the excitation/photon from the metal NP) predicts this behavior around the crossover at ( $\approx 150$  K), and the enhancement factor decreases as we move away from this point. In the theoretical analysis, it has been observed that accounting for the effect of increased decay rates on possible multiple excitations of the emitters helps to capture continuous laser excitation in the experimental systems, in contrast to a single excitation [28]. The PL intensity of AuNP-embedded QD systems is more sensitive to temperature changes than bare QDs, depending on the Debye temperature. This further suggests that by using fully absorbing plasmonic nanoparticles with higher Debye temperatures closer to room temperatures, it would be possible to develop highly efficient quantum dot based displays and devices. Nanoparticle-embedded QD assemblies have been used for low-temperature thermometry [75,76], by measuring PL intensity as a function of temperature. These types of materials have also been utilized for low-temperature sensing of other physical quantities such as magnetic fields, pressure, and strain due to their susceptible and selective responses to external perturbations, making them promising candidates for developing new sensors [77] with improved performance. We believe our results could have a significant impact in enhancing performance of

devices made from these materials in terms of their sensitivity and energy efficiency.

## V. CONCLUSION

In this study, we explored the temperature-dependent behavior of photoluminescence from compact quantum dot monolayer films embedded with tiny, fully absorbing gold nanoparticles. We observe significant photoluminescence enhancement at intermediate temperatures for the first time, which could be interpreted in terms of a non-Markovian approach to interactions between the emitters and metal nanoparticles. Furthermore, we found that the temperature dependence of the photoluminescence emission is driven by the relative strengths of the electron-electron and the electron-phonon interactions. The crossover temperature of approximately 150 K, where the radiative decay rate dominates over the dissipation, was found to be very close to the Debye temperature of gold nanoparticle. Our findings suggest that gold nanoparticle embedded quantum emitter films can improve the performance of nanophotonic devices, including displays and sensors, by tuning the system temperature offering potential strategies to improve emission efficiencies in such quantum emitter assemblies through temperature tuning.

## ACKNOWLEDGMENTS

We acknowledge the Department of Science and Technology (Nanomission) and SERB India for the financial support, and the Advanced Facility for Microscopy and Microanalysis (AFMM) Indian Institute of Science, Bangalore for the access to TEM measurements. R.D. acknowledges DST for financial support.

- 
- [1] C. R. Kagan, C. B. Murray, M. Nirmal, and M. G. Bawendi, Electronic energy transfer in cdse quantum dot solids, *Phys. Rev. Lett.* **76**, 1517 (1996).
  - [2] C. R. Kagan and C. B. Murray, Charge transport in strongly coupled quantum dot solids, *Nat. Nanotechnol.* **10**, 1013 (2015).
  - [3] W.-L. Ong, S. M. Rupich, D. V. Talapin, A. J. McGaughey, and J. A. Malen, Surface chemistry mediates thermal transport in three-dimensional nanocrystal arrays, *Nat. Mater.* **12**, 410 (2013).
  - [4] N. J. Halas, S. Lal, W.-S. Chang, S. Link, and P. Nordlander, Plasmons in strongly coupled metallic nanostructures, *Chem. Rev.* **111**, 3913 (2011).
  - [5] K. L. Kelly, E. Coronado, L. L. Zhao, and G. C. Schatz, The optical properties of metal nanoparticles: The influence of size, shape, and dielectric environment, *J. Phys. Chem. B* **107**, 668 (2003).
  - [6] N. S. Mueller, Y. Okamura, B. G. Vieira, S. Juergensen, H. Lange, E. B. Barros, F. Schulz, and S. Reich, Deep strong light-matter coupling in plasmonic nanoparticle crystals, *Nature (London)* **583**, 780 (2020).
  - [7] A. I. Kuznetsov, A. B. Evlyukhin, M. R. Gonçalves, C. Reinhardt, A. Koroleva, M. L. Arnedillo, R. Kiyan, O. Marti, and B. N. Chichkov, Laser fabrication of large-scale nanoparticle arrays for sensing applications, *ACS Nano* **5**, 4843 (2011).
  - [8] H. Hapuarachchi, S. Mallawaarachchi, H. T. Hattori, W. Zhu, and M. Premaratne, Optoelectronic figure of merit of a metal nanoparticle-quantum dot (mnp-qd) hybrid molecule for assessing its suitability for sensing applications, *J. Phys.: Condens. Matter* **30**, 054006 (2018).
  - [9] D. Sarkar, X. Xie, J. Kang, H. Zhang, W. Liu, J. Navarrete, M. Moskovits, and K. Banerjee, Functionalization of transition metal dichalcogenides with metallic nanoparticles: Implications for doping and gas-sensing, *Nano Lett.* **15**, 2852 (2015).
  - [10] M. Pelton, Modified spontaneous emission in nanophotonic structures, *Nat. Photonics* **9**, 427 (2015).
  - [11] V. Giannini, A. I. Fernández-Domínguez, S. C. Heck, and S. A. Maier, Plasmonic nanoantennas: Fundamentals and their use in controlling the radiative properties of nanoemitters, *Chem. Rev.* **111**, 3888 (2011).
  - [12] D. G. Baranov, R. S. Savelev, S. V. Li, A. E. Krasnok, and A. Alù, Modifying magnetic dipole spontaneous emission with nanophotonic structures, *Laser Photonics Rev.* **11**, 1600268 (2017).
  - [13] E. Yablonovitch, Inhibited spontaneous emission in solid-state physics and electronics, *Phys. Rev. Lett.* **58**, 2059 (1987).

- [14] D.-H. Kim, A. D'Aléo, X.-K. Chen, A. D. Sandanayaka, D. Yao, L. Zhao, T. Komino, E. Zaborova, G. Canard, Y. Tsuchiya *et al.*, High-efficiency electroluminescence and amplified spontaneous emission from a thermally activated delayed fluorescent near-infrared emitter, *Nat. Photonics* **12**, 98 (2018).
- [15] O. Painter, R. Lee, A. Scherer, A. Yariv, J. O'Brien, P. Dapkus, and I. Kim, Two-dimensional photonic band-gap defect mode laser, *Science* **284**, 1819 (1999).
- [16] S. Noda, M. Fujita, and T. Asano, Spontaneous-emission control by photonic crystals and nanocavities, *Nat. Photonics* **1**, 449 (2007).
- [17] R. Esteban, T. V. Teperik, and J.-J. Greffet, Optical patch antennas for single photon emission using surface plasmon resonances, *Phys. Rev. Lett.* **104**, 026802 (2010).
- [18] V. S. C. M. Rao and S. Hughes, Single quantum dot spontaneous emission in a finite-size photonic crystal waveguide: Proposal for an efficient "on chip" single photon gun, *Phys. Rev. Lett.* **99**, 193901 (2007).
- [19] J. A. Schuller, E. S. Barnard, W. Cai, Y. C. Jun, J. S. White, and M. L. Brongersma, Plasmonics for extreme light concentration and manipulation, *Nat. Mater.* **9**, 193 (2010).
- [20] D. Citrin, Y. Wang, and Z. Zhou, Far-field optical coupling to semi-infinite metal-nanoparticle chains, *J. Opt. Soc. Am. B* **25**, 937 (2008).
- [21] R. Bardhan, N. K. Grady, J. R. Cole, A. Joshi, and N. J. Halas, Fluorescence enhancement by Au nanostructures: Nanoshells and nanorods, *ACS Nano* **3**, 744 (2009).
- [22] D. Kim, H. Yokota, T. Taniguchi, and M. Nakayama, Precise control of photoluminescence enhancement and quenching of semiconductor quantum dots using localized surface plasmons in metal nanoparticles, *J. Appl. Phys.* **114**, 154307 (2013).
- [23] H. C. Park, Isnaeni, S. Gong, and Y.-H. Cho, How effective is plasmonic enhancement of colloidal quantum dots for color-conversion light-emitting devices? *Small* **13**, 1701805 (2017).
- [24] M. Haridas and J. K. Basu, Controlled photoluminescence from self-assembled semiconductor-metal quantum dot hybrid array films, *Nanotechnology* **21**, 415202 (2010).
- [25] M. Haridas, J. K. Basu, D. J. Gosztola, and G. P. Wiederrecht, Photoluminescence spectroscopy and lifetime measurements from self-assembled semiconductor-metal nanoparticle hybrid arrays, *Appl. Phys. Lett.* **97**, 083307 (2010).
- [26] K. A. Kang, J. Wang, J. B. Jasinski, and S. Achilefu, Fluorescence manipulation by gold nanoparticles: From complete quenching to extensive enhancement, *J. Nanobiotechnol.* **9**, 16 (2011).
- [27] M. Haridas, J. K. Basu, A. Tiwari, and M. Venkatapathi, Photoluminescence decay rate engineering of CdSe quantum dots in ensemble arrays embedded with gold nano-antennae, *J. Appl. Phys.* **114**, 064305 (2013).
- [28] R. Dutta, K. Jain, M. Venkatapathi, and J. K. Basu, Large emission enhancement and emergence of strong coupling with plasmons in nanoassemblies: Role of quantum interactions and finite emitter size, *Phys. Rev. B* **100**, 155413 (2019).
- [29] E. M. Thomas, C. L. Cortes, L. Paul, S. K. Gray, and K. G. Thomas, Combined effects of emitter-emitter and emitter-plasmonic surface separations dictate photoluminescence enhancement in a plasmonic field, *Phys. Chem. Chem. Phys.* **24**, 17250 (2022).
- [30] A. Kawabata and R. Kubo, Electronic properties of fine metallic particles. ii. plasma resonance absorption, *J. Phys. Soc. Jpn.* **21**, 1765 (1966).
- [31] F. Fujimoto and K.-i. Komaki, Plasma oscillations excited by a fast electron in a metallic particle, *J. Phys. Soc. Jpn.* **25**, 1679 (1968).
- [32] R. Ruppin, Decay of an excited molecule near a small metal sphere, *J. Chem. Phys.* **76**, 1681 (1982).
- [33] G. S. Agarwal and S. V. O'Neil, Effect of hydrodynamic dispersion of the metal on surface plasmons and surface-enhanced phenomena in spherical geometries, *Phys. Rev. B* **28**, 487 (1983).
- [34] V. M. Agranovich and V. Ginzburg, *Crystal Optics with Spatial Dispersion, and Excitons* (Springer, Berlin, Heidelberg, 1984).
- [35] U. Kreibig and M. Vollmer, *Optical Properties of Metal Clusters* (Springer, Berlin, Heidelberg, 1995).
- [36] J. A. Scholl, A. L. Koh, and J. A. Dionne, Quantum plasmon resonances of individual metallic nanoparticles, *Nature (London)* **483**, 421 (2012).
- [37] H.-P. Breuer and F. Petruccione, *The Theory of Open Quantum Systems* (Oxford University Press, Oxford, 2007), p. 656.
- [38] M. M. Wolf, J. Eisert, T. S. Cubitt, and J. I. Cirac, Assessing non-markovian quantum dynamics, *Phys. Rev. Lett.* **101**, 150402 (2008).
- [39] A. Rivas, S. F. Huelga, and M. B. Plenio, Entanglement and non-Markovianity of quantum evolutions, *Phys. Rev. Lett.* **105**, 050403 (2010).
- [40] H.-P. Breuer, E.-M. Laine, J. Piilo, and B. Vacchini, Colloquium: Non-markovian dynamics in open quantum systems, *Rev. Mod. Phys.* **88**, 021002 (2016).
- [41] K. H. Madsen, S. Ates, T. Lund-Hansen, A. Löffler, S. Reitzenstein, A. Forchel, and P. Lodahl, Observation of non-markovian dynamics of a single quantum dot in a micropillar cavity, *Phys. Rev. Lett.* **106**, 233601 (2011).
- [42] D. M. Kennes, O. Kashuba, M. Pletyukhov, H. Schoeller, and V. Meden, Oscillatory dynamics and non-markovian memory in dissipative quantum systems, *Phys. Rev. Lett.* **110**, 100405 (2013).
- [43] G. Agarwal, *Quantum Optics* (Cambridge University Press, Cambridge, England, 2013).
- [44] A. Gonzalez-Tudela, F. J. Rodríguez, L. Quiroga, and C. Tejedor, Dissipative dynamics of a solid-state qubit coupled to surface plasmons: From non-markov to markov regimes, *Phys. Rev. B* **82**, 115334 (2010).
- [45] C.-J. Yang and J.-H. An, Suppressed dissipation of a quantum emitter coupled to surface plasmon polaritons, *Phys. Rev. B* **95**, 161408(R) (2017).
- [46] A. Ishizaki and G. R. Fleming, Unified treatment of quantum coherent and incoherent hopping dynamics in electronic energy transfer: Reduced hierarchy equation approach, *J. Chem. Phys.* **130**, 234111 (2009).
- [47] K. Jain and M. Venkatapathi, Strong coupling of an emitter with absorbing matter: A regime for enhancement of light emission, *Phys. Rev. Appl.* **11**, 054002 (2019).
- [48] K. Jain and M. Venkatapathi, Role of Rabi oscillations in radiative states due to the fully absorbing smaller plasmonic nanoparticles, *J. Appl. Phys.* **132**, 113103 (2022).
- [49] K. Jain and M. Venkatapathi, Radiative decay of an emitter due to non-Markovian interaction with dissipating matter, *J. Phys.: Condens. Matter* **34**, 265302 (2022).

- [50] A. O. Govorov, G. W. Bryant, W. Zhang, T. Skeini, J. Lee, N. A. Kotov, J. M. Slocik, and R. R. Naik, Exciton-plasmon interaction and hybrid excitons in semiconductor-metal nanoparticle assemblies, *Nano Lett.* **6**, 984 (2006).
- [51] M. Praveena, A. Mukherjee, M. Venkatapathi, and J. K. Basu, Plasmon-mediated emergence of collective emission and enhanced quantum efficiency in quantum dot films, *Phys. Rev. B* **92**, 235403 (2015).
- [52] A. I. Frenkel, R. Vasić, B. Dukesz, D. Li, M. Chen, L. Zhang, and T. Fujita, Thermal properties of nanoporous gold, *Phys. Rev. B* **85**, 195419 (2012).
- [53] P. Mishra and B. K. Pandey, Variation of Debye temperature with size of nanoparticles, in *AIP Conference Proceedings*, edited by M. S. Shekhawat, S. Bhardwaj, and B. Suthar (AIP Publishing LLC, Bikaner, India, 2020), Vol. 2220, p. 020061.
- [54] M. Haridas, L. N. Tripathi, and J. K. Basu, Photoluminescence enhancement and quenching in metal-semiconductor quantum dot hybrid arrays, *Appl. Phys. Lett.* **98**, 063305 (2011).
- [55] See Supplemental Material at <http://link.aps.org/supplemental/10.1103/PhysRevMaterials.7.105201> for more details on the sample preparation, characterization, theoretical methods, and related additional figures.
- [56] B. Hecht, H. Bielefeldt, L. Novotny, Y. Inoué, and D. W. Pohl, Local excitation, scattering, and interference of surface plasmons, *Phys. Rev. Lett.* **77**, 1889 (1996).
- [57] M. Praveena, T. Phanindra Sai, R. Dutta, A. Ghosh, and J. K. Basu, Electrically tunable enhanced photoluminescence of semiconductor quantum dots on graphene, *ACS Photonics* **4**, 1967 (2017).
- [58] M. Praveena, R. Dutta, and J. K. Basu, Resonant enhancement of photoluminescence intensity and anisotropy of quantum dot monolayers with self-assembled gold nanorods, *Plasmonics* **12**, 1911 (2017).
- [59] R. Dutta, S. Kakkar, P. Mondal, N. Chauhan, and J. K. Basu, Electrical tuning of optical properties of quantum dot-graphene hybrid devices: Interplay of charge and energy transfer, *J. Phys. Chem. C* **125**, 8314 (2021).
- [60] R. Dutta, A. Pradhan, P. Mondal, S. Kakkar, T. P. Sai, A. Ghosh, and J. K. Basu, Enhancing carrier diffusion length and quantum efficiency through photoinduced charge transfer in layered graphene-semiconducting quantum dot devices, *ACS Appl. Mater. Interfaces* **13**, 24295 (2021).
- [61] J.-S. G. Bouillard, W. Dickson, D. P. O'Connor, G. A. Wurtz, and A. V. Zayats, Low-temperature plasmonics of metallic nanostructures, *Nano Lett.* **12**, 1561 (2012).
- [62] E. M. Purcell and C. R. Pennypacker, Scattering and absorption of light by nonspherical dielectric grains, *Astrophys. J.* **186**, 705 (1973).
- [63] B. T. Draine and P. J. Flatau, Discrete-dipole approximation for scattering calculations, *J. Opt. Soc. Am. A* **11**, 1491 (1994).
- [64] A. A. Svidzinsky, J. T. Chang, and M. O. Scully, Cooperative spontaneous emission of N atoms: Many-body eigenstates, the effect of virtual Lamb shift processes, and analogy with radiation of N classical oscillators, *Phys. Rev. A* **81**, 053821 (2010).
- [65] R. Wiegner, J. Von Zanthier, and G. S. Agarwal, Quantum-interference-initiated superradiant and subradiant emission from entangled atoms, *Phys. Rev. A* **84**, 023805 (2011).
- [66] D. Craig and T. Thirunamachandran, *Molecular Quantum Electrodynamics: An Introduction to Radiation-molecule Interactions*, Dover Books on Chemistry Series (Dover Publications, Mineola, New York, 1998).
- [67] D. S. Citrin, Coherent excitation transport in metal nanoparticle chains, *Nano Lett.* **4**, 1561 (2004).
- [68] V. N. Pustovit and T. V. Shahbazyan, Plasmon-mediated superradiance near metal nanostructures, *Phys. Rev. B* **82**, 075429 (2010).
- [69] E. B. Barros, B. G. Vieira, N. S. Mueller, and S. Reich, Plasmon polaritons in nanoparticle supercrystals: Microscopic quantum theory beyond the dipole approximation, *Phys. Rev. B* **104**, 035403 (2021).
- [70] N. Korsunskaya, M. Dybiec, L. Zhukov, S. Ostapenko, and T. Zhukov, Reversible and non-reversible photo-enhanced luminescence in CdSe/ZnS quantum dots, *Semicond. Sci. Technol.* **20**, 876 (2005).
- [71] D. Valerini, A. Creti, M. Lomascolo, L. Manna, R. Cingolani, and M. Anni, Temperature dependence of the photoluminescence properties of colloidal CdSe/ZnS core/shell quantum dots embedded in a polystyrene matrix, *Phys. Rev. B* **71**, 235409 (2005).
- [72] P. Jing, J. Zheng, M. Ikezawa, X. Liu, S. Lv, X. Kong, J. Zhao, and Y. Masumoto, Temperature-dependent photoluminescence of CdSe-core CdS/CdZnS/ZnS-multishell quantum dots, *J. Phys. Chem. C* **113**, 13545 (2009).
- [73] G. W. Walker, V. C. Sundar, C. M. Rudzinski, A. W. Wun, M. G. Bawendi, and D. G. Nocera, Quantum-dot optical temperature probes, *Appl. Phys. Lett.* **83**, 3555 (2003).
- [74] Y. P. Varshni, Temperature dependence of the energy gap in semiconductors, *Physica* **34**, 149 (1967).
- [75] C. Bradac, S. F. Lim, H.-C. Chang, and I. Aharonovich, Optical nanoscale thermometry: From fundamental mechanisms to emerging practical applications, *Adv. Opt. Mater.* **8**, 2000183 (2020).
- [76] N. S. Karan, A. M. Keller, S. Sampat, O. Roslyak, A. Arefin, C. J. Hanson, J. L. Casson, A. Desireddy, Y. Ghosh, A. Piryatinski *et al.*, Plasmonic giant quantum dots: Hybrid nanostructures for truly simultaneous optical imaging, photothermal effect and thermometry, *Chem. Sci.* **6**, 2224 (2015).
- [77] O. Benson, Assembly of hybrid photonic architectures from nanophotonic constituents, *Nature (London)* **480**, 193 (2011).